

## Highly efficient iron(0) nanoparticle-catalyzed hydrogenation in water in flow†

Cite this: *Green Chem.*, 2013, **15**, 2141

Reuben Hudson,<sup>a,b,c</sup> Go Hamasaka,<sup>b</sup> Takao Osako,<sup>b</sup> Yoichi M. A. Yamada,<sup>c</sup> Chao-Jun Li,<sup>a</sup> Yasuhiro Uozumi<sup>\*b,c</sup> and Audrey Moores<sup>\*a</sup>

Highly efficient catalytic hydrogenations are achieved by using amphiphilic polymer-stabilized Fe(0) nanoparticle (Fe NP) catalysts in ethanol or water in a flow reactor. Alkenes, alkynes, aromatic imines and aldehydes were hydrogenated nearly quantitatively in most cases. Aliphatic amines and aldehydes, ketone, ester, arene, nitro, and aryl halide functionalities are not affected, which provides an interesting chemoselectivity. The Fe NPs used in this system are stabilized and protected by an amphiphilic polymer resin, providing a unique system that combines long-term stability and high activity. The NPs were characterized by TEM of microtomed resin, which established that iron remains in the zero-valent form despite exposure to water and oxygen. The amphiphilic resin-supported Fe(0) nanoparticles in water and in flow provide a novel, robust, cheap and environmentally benign catalyst system for chemoselective hydrogenations.

Received 26th April 2013,  
Accepted 13th June 2013

DOI: 10.1039/c3gc40789f

[www.rsc.org/greenchem](http://www.rsc.org/greenchem)

### Introduction

Hydrogenation, known to chemists for decades, remains one of the most studied reactions. Its industrial applications span petrochemical conversion to pharmaceuticals synthesis; a plethora of catalysts exists for this transformation. However, hydrogenation reactions heavily rely on the chemistry of group 9 and 10 metals.<sup>1</sup> These elements are very expensive and their price is highly volatile on the stock market.<sup>2</sup> Regulatory organizations, such as the FDA, limit residual levels in pharmaceutical products to ppm or less levels because of their inherent toxicity. In response to these economic, regulatory and environmental concerns, efforts have been made to improve recovery and limit leaching,<sup>3</sup> or to seek metal-free solutions.<sup>4,5</sup> Iron has also been at the centre of renewed interest in both homogeneous and heterogeneous hydrogenation.<sup>6,7</sup> Iron complexes can catalyse the hydrogenation of alkenes,<sup>8,9</sup> carbonyls,<sup>6,10,11</sup> imines,<sup>11</sup> carbonates<sup>12</sup> in addition to the selective hydrogenation of alkynes to alkenes,<sup>13,14</sup> but such systems have limited recoverability. In contrast, heterogeneous catalysts are more amenable to recycling,<sup>15</sup> and several groups turned to

iron-based nanoparticles (NPs).<sup>16–19</sup> The de Vries group used soluble Fe NPs for hydrogenation of alkenes and alkynes,<sup>7,20</sup> while the Breit group functionalized graphene sheets with Fe NPs<sup>21</sup> to further aid recoverability and recycling. In these two systems, an accessible Fe(0) surface is responsible for the catalytic activity.<sup>22</sup> These two systems, however, exhibit great sensitivity to traces of either oxygen or water, thus limiting use in practical applications.

Over the past two decades, the use of water has gained considerable momentum as a solvent for organic reactions.<sup>23</sup> It enables novel reactivity,<sup>24,25</sup> speeds reactions by the hydrophobic<sup>26</sup> and 'on water' effects.<sup>27</sup> Ohde *et al.*<sup>28</sup> hydrogenated olefins with palladium nanoparticles in water-supercritical CO<sub>2</sub> microemulsions. More recently, Xiao *et al.* achieved asymmetric transfer of hydrogen 'on water'.<sup>29,30</sup> Amphiphilic polymers have also been used as supports for metal complexes and nanoparticles.<sup>31–33</sup> They are able to extract organic substrates from the aqueous phase resulting in higher concentrations near the catalyst, speeding the reaction. These systems demonstrate efficiency in hydrogenation,<sup>34–36</sup> oxidation,<sup>37,38</sup> cross coupling<sup>39</sup> and hydrodechlorination<sup>31,40,41</sup> reactions in water. The field of heterogeneous catalysis in water has been extensively reviewed.<sup>42</sup>

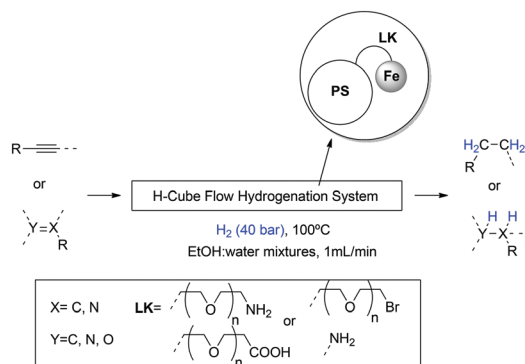
We recently demonstrated that core-shell iron/iron oxide nanoparticles are effective hydrogenation catalysts in protic media.<sup>43</sup> Exposure to oxygen and/or the presence of up to 1% of water does not affect catalytic activity, thanks to the protective effect of the iron oxide shell. However, neither pure nor water-rich mixtures could be used as a medium due to rapid catalyst deactivation. Additionally, the presence of the oxide

<sup>a</sup>Centre in Green Chemistry and Catalysis, Department of Chemistry, McGill University, 801 Sherbrooke St. West, Montreal, QC H3A 0B8, Canada. E-mail: [audrey.moores@mcgill.ca](mailto:audrey.moores@mcgill.ca)

<sup>b</sup>Division of Complex Catalysis, Institute for Molecular Science, Okazaki, 444-8787, Japan. E-mail: [uo@ims.ac.jp](mailto:uo@ims.ac.jp)

<sup>c</sup>RIKEN Center for Sustainable Resource Science, 2-1 Hirowasa, Wako, 351-0198, Japan

†Electronic supplementary information (ESI) available. See DOI: 10.1039/c3gc40789f



**Fig. 1** Schematic of hydrogenation reactions undertaken with polymer supported iron nanoparticles, under flow conditions (PS = polystyrene).

shell, although protective, limited access to the active surface and forced the use of more drastic conditions and longer reaction times.

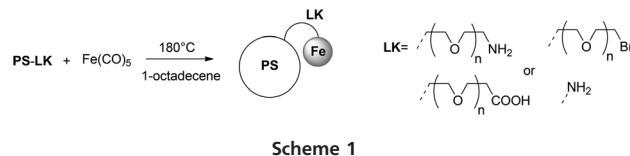
Building upon those initial results, we investigated supporting catalytically active Fe NPs on an amphiphilic polymer resin (Fig. 1). This combination provides the opportunity to use the catalyst in a flow system.<sup>44</sup> Flow systems are widely used to alleviate waste, work-up effort and scale-up problems.<sup>45,46</sup> Hydrogenation, in fact, has been one of the most researched reactions in flow systems because they allow to greatly reduce the volumes to pressurize, improving both gas consumption and safety.<sup>47–49</sup>

We herein report catalytic and selective hydrogenation of alkenes and alkynes, as well as aromatic imines and ketones, involving three green chemistry themes—flow chemistry, water as a benign solvent, and the use of cheap, non-toxic and biologically-essential heterogeneous iron (Fig. 1). By adapting known syntheses of reduced iron particles to the presence of a stabilizing polymer, we report the discovery of novel polymer supported iron nanoparticles that are uniquely robust toward oxidation, and yet active for hydrogenation catalysis. Quite remarkably, the polymer resin increased drastically the longevity of the nanoparticles, resulting in catalytic activity in ethanol and water–ethanol mixtures of up to 9 : 1. Interestingly, this method is very selective and specifically preserves aryl halide functionalities, a known limitation of palladium-based systems. In a demonstration of durability, scale-up of the system to 20 grams of substrate (styrene) can easily be achieved by increasing reaction time. Because this system is robust to water, iron can now be envisaged as a realistic competitor to platinum series metals as a practical hydrogenation catalyst.

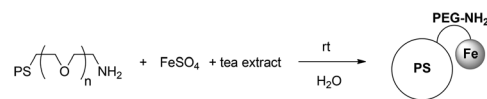
## Results and discussion

### Synthesis and characterization of polymer resin stabilized Fe(0) NPs

Amphiphilic polymer resins composed of polystyrene (PS) beads (average size 90 micron), functionalized with a variety of linkers (LK) were used to support Fe NPs (Fig. 1). The PS beads serve as compact supports, whose surfaces are covered with



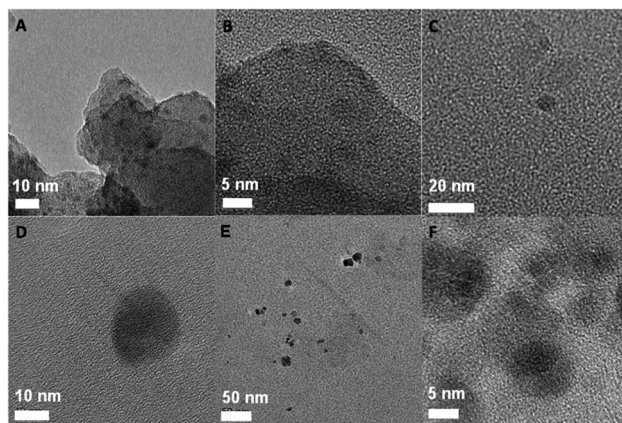
**Scheme 1**



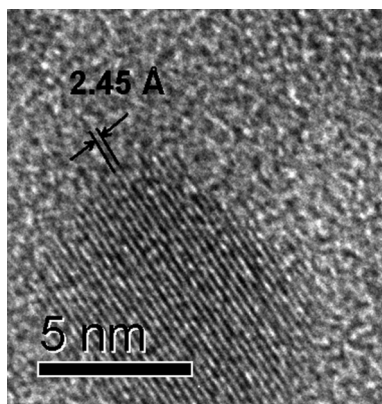
**Scheme 2**

LK-stabilized Fe NPs. These LKs are terminated with a functional group (FG = NH<sub>2</sub>, COOH, Br) and may also contain a polyethylene glycol (PEG) spacer. The Fe NPs were synthesized *in situ*, in the presence of the polymer. We adapted two known methods to produce our novel catalysts: (1) the thermal decomposition<sup>50,51</sup> of Fe(CO)<sub>5</sub> (Scheme 1); (2) the reduction of FeSO<sub>4</sub> using black tea as a reducer<sup>52</sup> (Scheme 2). The first method was expected to afford salt free, smaller and more reduced NPs than any other known method of Fe NPs production. The second synthesis proceeds *via* reduction of iron salts by tea polyphenols<sup>52</sup> and was selected as a green alternative to the first synthesis. The catalysts reported herein are notably different from already published methods in two notable ways. First, rather than using oleyamine, or other stabilizers, as a stabilizing agent, we use FG terminated PEGylated spacers, which likely passivate the nanoparticle surface (*vide infra*), dissuading formation of a surface oxide layer, as generally observed.<sup>50,51</sup> Second, because the polymer is present during the time of nanoparticle seeding and growth, it affords a robust resin that can be used in a flow system.

The resulting materials were characterized by transmission electron microscopy (TEM) of microtomed slices of the materials. This method allowed visualization of the Fe NPs embedded in the linker covering the PS beads (Fig. 2).



**Fig. 2** TEM images of images of (A) and (B) FeNP@PS-PEG-NH<sub>2</sub> (thermal decomposition); (C) FeNP@PS-PEG-NH<sub>2</sub> (tea reduction); (D) FeNP@PS-PEG-Br (thermal decomposition); (E) FeNP@PS-PEG-COOH (thermal decomposition); (F) FeNP@PS-NH<sub>2</sub> (thermal decomposition).



**Fig. 3** High resolution TEM image of a single Fe(0) NP exhibiting lattice fringes in FeNP@PS-PEG-NH<sub>2</sub>.

PS-(PEG)-NH<sub>2</sub> afforded the best results. Well dispersed and monodisperse ~5 nm Fe NPs were observed in the case of thermal decomposition (Fig. 2A and B). At high resolution, regular lines evince the crystal lattice of FeNP@PS-PEG-NH<sub>2</sub> (Fig. 3). The lines are separated by 2.45 Å, which is in good agreement with the interatomic spacing calculated to be 2.49 Å, from either bcc or fcc iron.<sup>53</sup> These are very different from spacing measured for iron oxides.<sup>54,55</sup> They demonstrate the Fe(0) nature of the nanoparticles. Fewer particles were visible when using the tea reduction method, most of them having again a size of ~5 nm (Fig. 2C). With both PS-(PEG)-Br and PS-(PEG)-COOH, the thermal decomposition afforded larger particles between 15 and 20 nm for Br and 5 and 20 nm for COOH. PS-NH<sub>2</sub> afforded localized clusters of particles between 5 and 10 nm. Large sections of the matrix did not contain Fe NPs. In no sample did we see any iron oxide layer at the surface of the particles, as we had observed in previous work.<sup>43</sup> This demonstrates the excellent stability of this system toward oxidation, presumably through a stabilizing effect of the polymeric support.

In addition to TEM, the materials were characterized by ICP (Table 1). The highest loading was obtained with FeNP@PS-PEG-NH<sub>2</sub> with 11.72 mg Fe g<sup>-1</sup> (entry 1), confirming the observation made by TEM. In terms of loading, thermal decomposition was a more efficient method than tea reduction as the latter afforded material with about 5 times less iron content (entry 2). Indeed, the reaction conditions of thermal decomposition, which occurs at 180 °C, were more favourable to iron diffusion, than those of tea reduction (room temperature). Additionally, the neutral nature of Fe(CO)<sub>5</sub> is more adapted to the PEGylated environment surrounding the PS beads than Fe<sup>2+</sup> salts. A change in the terminal group, from NH<sub>2</sub> to COOH (entry 3) or Br (entry 4) affected loading, although all PEGylated systems could successfully immobilize Fe NPs. Amines are classical Fe NPs stabilizers, used notably in the original synthesis of Fe NPs by thermal decomposition, and are expected to be better ligands than either -Br or -COOH functionalized polymers.<sup>38,39</sup> Removal of the PEG spacer while keeping the amine functionality (entry 5) had a

**Table 1** Ethylbenzene yield in batch and flow as a function of polymer-immobilized Fe NP composition

Entry	Composition	Fe loading <sup>a</sup>	Yield/flow <sup>b</sup> (%)	Yield/batch <sup>c</sup> (%)
1	FeNP@PS-PEG-NH <sub>2</sub> <sup>d</sup>	11.72	100	44
2	FeNP@PS-PEG-NH <sub>2</sub> <sup>e</sup>	2.55	100	13
3	FeNP@PS-PEG-COOH <sup>d</sup>	5.01	100	24
4	FeNP@PS-PEG-Br <sup>d</sup>	4.05	100	8
5	FeNP@PS-NH <sub>2</sub> <sup>d</sup>	1.03	100	19
6	PS-PEG-NH <sub>2</sub>	0	0	0
7	FeNP <sup>f</sup>	All iron	N/A <sup>g</sup>	26

<sup>a</sup> mg Fe g<sup>-1</sup> polymer determined by ICP. <sup>b</sup> Reaction conditions: 100 °C, 40 bar, 1 mL min<sup>-1</sup> through 300 mg polymer, 0.05 M styrene in EtOH (residence time 53 seconds). <sup>c</sup> Reactions conditions: 100 °C, 40 bar, 0.05 M styrene in EtOH (17 mL), 6 hours. <sup>d</sup> Fe nanoparticles generated by thermal decomposition of Fe(CO)<sub>5</sub>. <sup>e</sup> Fe nanoparticles generated by black tea-extract reduction of FeSO<sub>4</sub>. <sup>f</sup> Reaction conditions: 100 °C, 40 bar, 0.05 M styrene in EtOH (17 mL), 5 mol% FeNP (generated by thermal decomposition of Fe(CO)<sub>5</sub> with oleyamine as a stabilizer),<sup>50</sup> 6 hours. <sup>g</sup> The catalyst could not be tested in flow without polymer support.

drastic effect on loading with a 10 fold drop in Fe content, perhaps because the extra oxygen atoms help to coordinate iron, helping seed the formation of nanoparticles.

### Catalytic tests

These polymer supported-Fe NPs were then assessed in both flow and batch conditions for the hydrogenation of styrene in ethanol (Table 1). The flow system consists of a peristaltic pump that forces a solution of the solvent and substrate through a cartridge packed with the catalyst, heated and pressurized with H<sub>2</sub> gas.

All iron/polymer systems provided quantitative yields in the flow conditions. However, only the FeNP@PS-PEG-NH<sub>2</sub> generated by thermal decomposition provided even a moderate yield in batch conditions (Table 1, entry 1). Interestingly, the FeNP@PS-PEG-NH<sub>2</sub> produced using the tea extract method afforded a modest yield of 13% in batch conditions (entry 2), which is superior to what could be expected from simply considering the 5-fold lower loading from the thermal decomposition method. Replacement of the NH<sub>2</sub> functionality by COOH (entry 3) or Br (entry 4), or the removal of the PEG spacer (entry 5), afforded lower yields than FeNP@PS-PEG-NH<sub>2</sub>, presumably because of the lower loading. The excellent performance of all these systems in flow compared to batch conditions can be explained by the very high local catalyst concentration within the flow cell. Fe NPs were critical to catalysis, PS-PEG-NH<sub>2</sub> alone did not lead to any measurable conversion in the conditions used (Table 1, entry 6). Nanoparticles generated without the polymer support (and instead with oleyamine as a stabilizer) could be tested in batch conditions, but not in flow, because, with no support, they would not stay anchored in the flow system. Simple Fe NPs demonstrated a reasonable activity in batch conditions, as expected for small iron NPs (~12 nm)<sup>50</sup> protected from oxidation by air or water.<sup>7,43</sup> Consistent with these results, this reaction is

**Table 2** Screening of hydrogenation conditions<sup>a</sup>

Entry	Pressure (bar)	Temp (°C)	Flow (mL min <sup>-1</sup> )	Yield (%)	TOF (h <sup>-1</sup> )
1	40	100	2	92	106
2	60	100	2	95	109
3	20	100	2	85	97
4	40	100	1	100	57
5	40	100	0.5	94	26
6	10	100	1	54	30
9	40	80	1	95	54
10	40	60	1	94	53
11 <sup>b</sup>	40	100	1	100	57
12 <sup>c</sup>	40	100	1	95	54
13 <sup>d</sup>	40	100	1	88	50
14 <sup>e</sup>	40	100	1	0	0

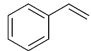
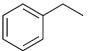

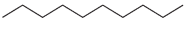




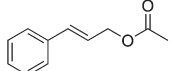
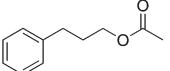
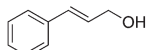
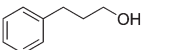
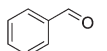
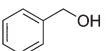
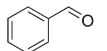
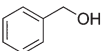
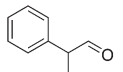
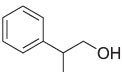
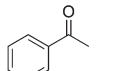
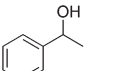
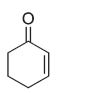
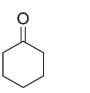
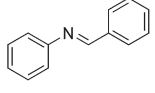
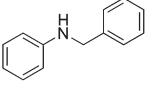
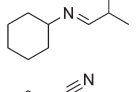
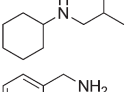
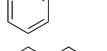
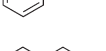
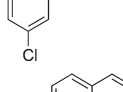
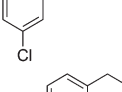
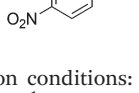
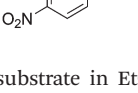
<sup>a</sup> Reaction conditions: styrene (0.05 M) in EtOH was circulated through 250 mg of FeNP@PS-PEG-NH<sub>2</sub> resin (generated by thermal decomposition of Fe(CO)<sub>5</sub>). <sup>b</sup> EtOH-H<sub>2</sub>O = 1:99 v:v. <sup>c</sup> EtOH-H<sub>2</sub>O = 50:50 v:v. <sup>d</sup> EtOH-H<sub>2</sub>O = 10:90 v:v. <sup>e</sup> No catalyst present.

expected to proceed through the classical heterogeneous hydrogenation mechanism (see ESI†). Based on these preliminary results, we used FeNP@PS-PEG-NH<sub>2</sub> generated by thermal decomposition in the rest of the study.

Selective hydrogenation of styrene double bond served as a model reaction for the optimization of reaction conditions (Table 2). Conditions of 40 bar H<sub>2</sub>, 100 °C and a flow rate of 2 mL min<sup>-1</sup> constituted the benchmark conditions, achieving a 92% yield of ethyl benzene (Table 2, entry 1). Increasing the pressure to 60 bar pushed the yield to 95% (Table 2, entry 2). Decreasing the flow rate to 1 mL min<sup>-1</sup> afforded a quantitative yield, by improving residence time on the catalyst (Table 2, entry 4). The reaction still proceeded to 95% yield in 50:50 ethanol-water (Table 2, entry 12), and an 88% yield in 10:90 ethanol-water (Table 2, entry 13).<sup>56</sup> This constitutes a great improvement compared to our previously reported iron/iron oxide core-shell system, where a 50:50 ethanol-water mixture significantly affected hydrogenation catalysis.<sup>43</sup> The increased stability of the Fe NPs in a 90% water medium arises from the embedding of the particles in lipophilic pockets of the polymers, preventing water oxidation of their surface. Both Fe(0) NP syntheses tested – namely the thermal decomposition of Fe(CO)<sub>5</sub> and the greener black tea extract reduction of FeSO<sub>4</sub> – afforded quantitative yields under benchmark conditions (40 bar, *T* = 100 °C, 2 mL min<sup>-1</sup>, with PS-PEG-NH<sub>2</sub> resin) (Table 1). FeNP@PS-PEG-COOH, FeNP@PS-PEG-Br, FeNP@PS-NH<sub>2</sub> were also equally efficient under the same conditions (Table 1).

We performed ICP analysis of the digested catalysts and could not detect any other metal, not even nickel, a common contaminant of iron known to be active for hydrogenation. This result is consistent with the fact that Fe(CO)<sub>5</sub> purity is claimed to be 99.999%. This demonstrates that the catalytic activity measured originates solely from iron. Additionally, ICP analysis of the product solution indicated only 0.007 ppm soluble iron strongly suggesting a heterogeneous mechanism.

**Table 3** Functional group tolerance and selectivity<sup>a</sup>

Entry	Substrate	Product	Yield-selectivity (%-%)
1			100-100
2			73-91
3			67-100
4			79-87
5			98-100
6			100-100
7			35-96
8 <sup>b</sup>			85-98
9			0-N/A
10			0-N/A
11			100-100
12			100-100
13			0-N/A
14			0-N/A
15			99-100
16			84-100

<sup>a</sup> Reaction conditions: 0.05 M substrate in EtOH, 100 °C, 40 bar H<sub>2</sub>, 1 mL min<sup>-1</sup>, 300 mg FeNP@PS-PEG-NH<sub>2</sub> (residence time 53 seconds).

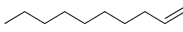
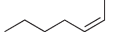
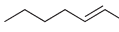
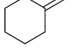
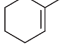
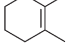
<sup>b</sup> Reaction conditions: 0.05 M substrate in EtOH, 100 °C, 60 bar H<sub>2</sub>, 1 mL min<sup>-1</sup> 300 mg FeNP@PS-PEG-NH<sub>2</sub> (residence time 53 seconds).

With optimized conditions in hand, functional group tolerance and selectivity was explored (Table 3). The catalyst system is highly active for aromatic alkene hydrogenation (entries 1, 5, 15 and 16). The catalytic conditions are moderately efficient toward aliphatic alkenes (entry 3) and alkynes, both internal (entry 4) and terminal (entry 2). The system demonstrates selectivity for C-C double and triple bonds over ketones (Table 3, entries 6 and 11), esters (entry 5), nitriles (entry 14), arenes (entries 1, 5, 6, 15, and 16). The system also selects against aliphatic aldehydes (entry 9) and imines (entry 13).

**Table 4** Catalytic selectivity of the polymer-immobilized Fe NPs

Substrate	Catalytic conversion
Alkenes and alkynes	Yes
Aldehydes and imines	Yes for aromatic, no for aliphatic
Ketone, ester, nitro, arene, benzyl carbamate, reductive elimination of aryl halides	No

**Table 5** Reactivity of various types of alkenes<sup>a</sup>

Entry	Substrate	Yield (%)
1		90
2		87
3		83
4		14
5		6
6		Trace

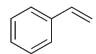
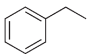
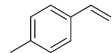
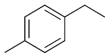
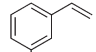
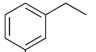
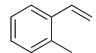
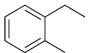
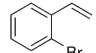
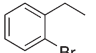
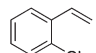
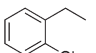
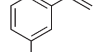
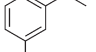
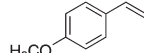
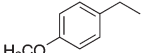
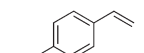
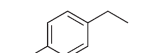
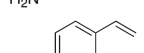
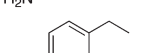
<sup>a</sup> Reaction conditions: 40 bar H<sub>2</sub>, 100 °C, 0.5 mL min<sup>-1</sup>, 0.05 M substrate in EtOH (residence time 116 seconds).

When activated by an aromatic ring, however, aldehydes (entries 7 and 8) and imines (entry 12) react. The greater activity demonstrated by aromatic activated substrates relative to their aliphatic analogues could be attributed to the lower LUMO of the former relative to the latter. The reductive elimination of aryl halides (entry 15) or reduction of nitro groups (entry 16) does not occur under these mild conditions—opening the doors for selective synthesis. Given the sensitivity of aryl halides and aryl nitro groups to reducing conditions with platinum series catalysts,<sup>57</sup> these two examples of chemoselectivity open a land of opportunities in synthesis. A summary of observed chemoselectivity is provided in Table 4.

Various substituted, non-functionalized alkenes were assessed (Table 5). The flow speed was divided by 2 because such alkenes, when not activated by an aromatic ring, are less reactive (see Table 3, entries 1 and 3). Hydrogenation of mono-substituted alkenes (Table 5, entry 1) proceeds in good yields, *cis* alkenes (Table 5, entry 2) reacted slightly faster than *trans* alkenes (Table 5, entry 3). Geminal substitution is more problematic (Table 5, entry 4). Considering this, it is not surprising that tri-substituted alkenes (Table 5, entry 5) reacted exceptionally slowly and tetra-substituted alkenes exhibit negligible reactivity (Table 5, entry 6). Although the greater degree of substitution would electronically favour hydrogenation in these substrates over the less substituted analogue, the reverse reactivity can be attributed with the difficulty of coordinating more sterically hindered substrates to a heterogeneous surface.

For the sake of comparing the reactivity of various styrene derivatives, we used milder reaction conditions in order to

**Table 6** Activity of styrene derivatives<sup>a</sup>

Entry	Substrate	Product	Yield (%)	Selectivity (%)
1			45	>99
2			52	>99
3			48	>99
4			42	>99
5			18	>99
6			35	>99
7			58	>99
8			54	>99
9			50	>99
10			39	>99

<sup>a</sup> Reaction conditions: 0.05 M substrate in EtOH, 80 °C, 20 bar H<sub>2</sub>, 3 mL min<sup>-1</sup>, 300 mg FeNP@PS-PEG-NH<sub>2</sub> (residence time 18 seconds).

achieve greater separation of chemical yields (Table 6). This comparison suggests that sterics affect reactivity more than electronics. For example, the difference in yield between *ortho* (entry 6, 35%) and *meta* (entry 7, 58%) chloro substituted styrene overshadows the difference in yield between electron donating (NH<sub>2</sub>, entry 9, 50%) and electron withdrawing (NO<sub>2</sub>, entry 10, 39%) *para* substituted styrene. The trend for methylstyrene further demonstrates this effect. *para* Methylstyrene (entry 2, 52%) and *meta*-methylstyrene (entry 3, 48%) both reacted faster than unsubstituted styrene (entry 1, 45%). However, *ortho*-methylstyrene reacts slower (entry 2, 42%). Once in the *ortho* position, the negative steric effect of the methyl group outweighs the positive electron-donating effect. It is therefore not surprising that the example with the largest *ortho* substituent (Br, entry 5) exhibits the lowest overall yield (18%). For each entry in Table 6, no side products were observed.

Ease of reaction scale-up represents one of the most attractive benefits of flow chemistry. We therefore performed a scale-up test and hydrogenated five grams of cinnamyl acetate (Fig. 4) in the course of 5.7 hours. This experiment demonstrated the robust nature of the catalyst in prolonged reactions. The hourly snapshots indicate that the yield incrementally decreased from 97% to 94%; this very modest yield decrease may be caused by several factors, including a slight oxidation of the Fe NPs or an excessive packing of the catalyst beads over

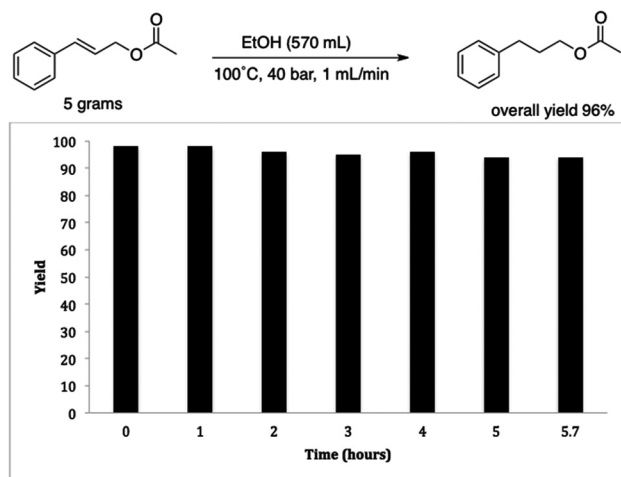


Fig. 4 Scale up and long-term catalyst performance for the hydrogenation of 5 grams of cinnamyl acetate over 5.7 hours (TON = 434).

time. This equates to a turn over number (TON) of 434. In another scale-up experiment, we fed the system with 20.7 gram of styrene over 29 hours, and obtained a total TON of 1685.

In conclusion, we describe a novel synthesis of polymer supported Fe NPs, which display excellent reactivity for the selective hydrogenation of alkenes, alkynes, aromatic imines and aldehydes in a flow system. The catalyst is robust in the presence of water, surpassing hydrogenation reaction yields for aqueous mixtures of all other iron nanoparticle systems reported to date.<sup>7,43</sup> Very interesting selectivity was achieved and complete protection of the sensitive aryl halides during hydrogenation is an important progress provided by the novel catalysts presented herein. This catalytic flow system functions well at the multi gram scale. This work reports for the first time the convergence of three green chemistry conditions: flow hydrogenation with H<sub>2</sub>, use of water and ethanol as benign solvents and the use of heterogeneous iron as a catalyst. More importantly, it opens the possibility of using iron as a replacement to platinum series metals for hydrogenation reaction under realistic, industrial conditions. Current efforts in our labs are focused on achieving a better understanding of the stability of this system toward oxidation and of the mechanism of the reaction.

## Experimental section

### Chemicals

Styrene (99.0% w/~0.003% *p*-*t*-butylcatechol stabilizer) and *p*-methoxystyrene (99% w/200 ppm *p*-*t*-butylcatechol stabilizer) were purchased from Wako Chemicals. Cinnamyl alcohol (98.0%), *trans*-2-heptene (99%), *cis*-2-heptene (97%), Fe(CO)<sub>5</sub> (99.999%) and 1-octadecene (90%) were purchased from Aldrich. 2-Phenylpropionaldehyde (98%), cinnamyl acetate (99%), 4-methylstyrene (99%), benzylideneaniline (98%), and benzylcarbamate (97%) were purchased from TCI. Ethanol (99.5%) was purchased from Kanto Chemical Co. Tentagel

S COOH, Tentagel S Br and Tentagel S NH<sub>2</sub> were purchased from RAPP Polymere (Germany). Aminomethylated polystyrene was purchased from Nova Biochem (Germany). High purity water was obtained by the use of a Milli-Q-Millipore with 0.22 μm filter, Q-guard1 and an ultrapure organex cartridge.

### Instruments

An Agilent Technologies 6850 series II Network GC System, fitted with a flame ionization detector (GC FID). The GC MS was an Agilent 5973 Network Mass Selective Detector. High pressure hydrogenation flow reactor catalytic tests were performed on an H-Cube (Thales Nanotechnologies). The transmission electron microscope (TEM) used for imaging was a JEM-2010F (HR7). Microtome slices were prepared using a Leica EMFCS. The inductively coupled plasma (ICP) measurements were recorded on a Leeman labs, inc. Profile Plus high dispersion ICP.

### Synthesis of FeNP@PS-LK by thermal decomposition

Linker-terminated polystyrene/(polyethylene glycol) beads (Tentagel from RAPP Polymere or aminomethylated polystyrene from Nova, 1 gram) and 1-octadecene (60 mL, 90% Aldrich) were combined with a magnetic stir bar in a 200 mL round bottom Schlenk flask. The mixture was purged with N<sub>2</sub> at 120 °C for 30 minutes. The temperature was then raised to 180 °C, at which point Fe(CO)<sub>5</sub> (2.1 mL, 99.99%, Aldrich) was quickly injected. The reaction was stirred for 30 minutes at 180 °C under a blanket of N<sub>2</sub>, then allowed to cool to room temperature. The resulting polymer-supported iron nanoparticles (FeNP@PS-(PEG)-FG) were washed 3 times with hexanes (50 mL, 99% Aldrich) and dried under vacuum.

### Synthesis of FeNP@PS-(PEG)-NH<sub>2</sub> by black tea reduction

Red Label black tea (20 g) was brewed with boiling water (1 L) and cooled to room temperature. The brewed tea was then added to a solution of amine-terminated polystyrene/polyethylene glycol beads (1 gram), FeSO<sub>4</sub> (3.767 g) and water (2 L) with a magnetic stir bar in a 4 L glass jug. After stirring for 24 hours, the polymer was filtered and collected.

### Characterization of PS-LK supported Fe nanoparticles

To visualize the FeNP@PS-(PEG)-FG catalysts, the polymer was sliced with a Leica EMFCS microtome. The resulting slices were loaded onto carbon/Formvar grids and subjected to TEM analysis on a JEM-2010F (HR7) operated at 120 kV. The interatomic spacing was measured on Fig. 3 using the measuring tool of the GIMP software over 14 lines. The lattice parameter is 2.87 Å for bcc iron and 3.515 Å for fcc,<sup>53</sup> and thus an interatomic spacing of 2.49 Å.

### PS-LK supported Fe nanoparticles for flow hydrogenation

A cartridge packed with 300 mg of PS-LK supported Fe nanoparticles was connected to an H-Cube flow hydrogenation system. Each substrate (0.05 M) in ethanol, water, or a mixture of the two was forced through the system at different rates,

temperatures and hydrogen pressures. The resulting solution was characterized by GC-MS and quantified by GC-FID.

### PS-LK supported Fe nanoparticles for batch hydrogenation

High pressure batch reactions were performed in a Parr 5000 high pressure multireactor with 17 mL of 0.05 M styrene in EtOH and a magnetic stirbar (1000 rpm) for 6 hours with 300 mg of polymer-supported catalyst. The reaction mixture was then filtered through a Buchner funnel and injected directly into a GC equipped with a flame ionization detector.

## Acknowledgements

We thank the Natural Science and Engineering Council of Canada (NSERC), the Canada Foundation for Innovation (CFI), the Canada Research Chairs (CRC), the Fonds de Recherche du Québec – Nature et Technologies (FRQNT), the Centre in Green Chemistry and Catalysis (CCGC), the Green Chemistry – NSERC Collaborative Research and Training Experience (CREATE) Program, the Riken-McGill fund, McGill University, JSPS (Grant-in-Aid for Scientific Research #20655035 and #24550126; Grant-in-Aid for Scientific Research on Innovative Areas #2105), the CREST program “Elemental Strategy” and JST ACT-C for their financial support. Lynn Leger (Green Centre Canada), Shatha Qaqish (Green Centre Canada), Bruce Lennox and Tomislav Friscic are thanked for their useful comments.

## Notes and references

- J. G. de Vries and C. J. Elsevier, *Handbook of Homogeneous Hydrogenation*, Wiley-VCH, Weinheim, 2007.
- A. Behr and P. Neubert, *Applied Homogeneous Catalysis*, Wiley-VCH, Weinheim, Germany, 2012.
- C. M. Crudden, M. Sateesh and R. Lewis, *J. Am. Chem. Soc.*, 2005, **127**, 10045–10050.
- P. A. Chase and D. W. Stephan, *Angew. Chem., Int. Ed.*, 2008, **47**, 7433–7437.
- P. A. Chase, T. Jurca and D. W. Stephan, *Chem. Commun.*, 2008, 1701–1703.
- R. H. Morris, *Chem. Soc. Rev.*, 2009, **38**, 2282–2291.
- P.-H. Phua, L. Lefort, J. A. F. Boogers, M. Tristany and J. G. de Vries, *Chem. Commun.*, 2009, 3747–3749.
- S. C. Bart, E. J. Hawrelak, E. Lobkovsky and P. J. Chirik, *Organometallics*, 2005, **24**, 5518–5527.
- S. C. Bart, E. Lobkovsky and P. J. Chirik, *J. Am. Chem. Soc.*, 2004, **126**, 13794–13807.
- A. Mikhailine, A. J. Lough and R. H. Morris, *J. Am. Chem. Soc.*, 2009, **131**, 1394–1395.
- C. Sui-Seng, F. Freutel, A. J. Lough and R. H. Morris, *Angew. Chem., Int. Ed.*, 2008, **47**, 940–943.
- C. Federsel, A. Boddien, R. Jackstell, R. Jennerjahn, P. J. Dyson, R. Scopelliti, G. Laurenczy and M. Beller, *Angew. Chem., Int. Ed.*, 2010, **49**, 9777–9780.
- S. Enthaler, M. Haberberger and E. Irran, *Chem.-Asian J.*, 2011, **6**, 1613–1623.
- M. Haberberger, E. Irran and S. Enthaler, *Eur. J. Inorg. Chem.*, 2011, 2797–2802.
- S. Shylesh, V. Schünemann and W. R. Thiel, *Angew. Chem., Int. Ed.*, 2010, **49**, 3428–3459.
- M. Armbruster, K. Kovnir, M. Friedrich, D. Teschner, G. Wowsnick, M. Hahne, P. Gille, L. Szentmiklosi, M. Feuerbacher, M. Heggen, F. Girgsdies, D. Rosenthal, R. Schlogl and Y. Grin, *Nat. Mater.*, 2012, **11**, 690–693.
- D. Cantillo, M. Baghbanzadeh and C. O. Kappe, *Angew. Chem., Int. Ed.*, 2012, **51**, 10190–10193.
- J. F. Sonnenberg, N. Coombs, P. A. Dube and R. H. Morris, *J. Am. Chem. Soc.*, 2012, **134**, 5893–5899.
- J.-M. Yan, X.-B. Zhang, S. Han, H. Shioyama and Q. Xu, *Angew. Chem., Int. Ed.*, 2008, **47**, 2287–2289.
- C. Rangheard, C. de Julian Fernandez, P.-H. Phua, J. Hoorn, L. Lefort and J. G. de Vries, *Dalton Trans.*, 2010, **39**, 8464–8471.
- M. Stein, J. Wieland, P. Steurer, F. Toelle, R. Muelhaupt and B. Breit, *Adv. Synth. Catal.*, 2011, **353**, 523–527.
- A. Welther, M. Bauer, M. Mayer and A. Jacobi von Wangelin, *ChemCatChem*, 2012, **4**, 1088–1093.
- C.-J. Li and T.-H. Chan, *Comprehensive Organic Reactions in Aqueous Media*, Wiley, 2007.
- C.-J. Li and L. Chen, *Chem. Soc. Rev.*, 2006, **35**, 68–82.
- C. J. Li, *Chem. Rev.*, 1993, **93**, 2023–2035.
- R. Breslow, *Acc. Chem. Res.*, 1991, **24**, 159–164.
- S. Narayan, J. Muldoon, M. G. Finn, V. V. Fokin, H. C. Kolb and K. B. Sharpless, *Angew. Chem., Int. Ed.*, 2005, **44**, 3275–3279.
- H. Ohde, C. M. Wai, H. Kim, J. Kim and M. Ohde, *J. Am. Chem. Soc.*, 2002, **124**, 4540–4541.
- X. Wu, X. Li, F. King and J. Xiao, *Angew. Chem.*, 2005, **117**, 3473–3477.
- X. Wu, J. Liu, X. Li, A. Zanotti-Gerosa, F. Hancock, D. Vinci, J. Ruan and J. Xiao, *Angew. Chem., Int. Ed.*, 2006, **45**, 6718–6722.
- Y. Uozumi and Y. M. A. Yamada, *Chem. Rec.*, 2009, **9**, 51–65.
- S. M. Sarkar, Y. Uozumi and Y. M. A. Yamada, *Angew. Chem.*, 2011, **123**, 9609–9613.
- Y. M. A. Yamada, S. M. Sarkar and Y. Uozumi, *J. Am. Chem. Soc.*, 2012, **134**, 3190–3198.
- M. T. Zarka, O. Nuyken and R. Weberskirch, *Chem.-Eur. J.*, 2003, **9**, 3228–3234.
- Y. Arakawa, A. Chiba, N. Haraguchi and S. Itsuno, *Adv. Synth. Catal.*, 2008, **350**, 2295–2304.
- Y. Uozumi and Y. M. A. Yamada, *Chem. Rec.*, 2009, **9**, 51–65.
- Y. Uozumi and R. Nakao, *Angew. Chem., Int. Ed.*, 2003, **42**, 194–197.
- Y. M. A. Yamada, T. Arakawa, H. Hocke and Y. Uozumi, *Chem.-Asian J.*, 2009, **4**, 1092–1098.
- C. B. Putta and S. Ghosh, *Adv. Synth. Catal.*, 2011, **353**, 1889–1896.

- 40 R. Nakao, H. Rhee and Y. Uozumi, *Org. Lett.*, 2004, **7**, 163–165.
- 41 Y. M. A. Yamada, T. Watanabe, A. Ohno and Y. Uozumi, *ChemSusChem*, 2012, **5**, 293–299.
- 42 M. Lamblin, L. Nassar-Hardy, J.-C. Hierso, E. Fouquet and F.-X. Felpin, *Adv. Synth. Catal.*, 2010, **352**, 33–79.
- 43 R. Hudson, A. Riviere, C. M. Cirtiu, K. L. Luska and A. Moores, *Chem. Commun.*, 2012, **48**, 3360–3362.
- 44 G. Jas and A. Kirschning, *Chem.–Eur. J.*, 2003, **9**, 5708–5723.
- 45 G. M. Whitesides, *Nature*, 2006, **442**, 368–373.
- 46 J. Wegner, S. Ceylan and A. Kirschning, *Chem. Commun.*, 2011, **47**, 4583–4592.
- 47 U. K. Singh and M. A. Vannice, *Appl. Catal., A*, 2001, **213**, 1–24.
- 48 J. Kobayashi, Y. Mori, K. Okamoto, R. Akiyama, M. Ueno, T. Kitamori and S. Kobayashi, *Science*, 2004, **304**, 1305–1308.
- 49 M. Ruta, G. Laurenczy, P. J. Dyson and L. Kiwi-Minsker, *J. Phys. Chem. C*, 2008, **112**, 17814–17819.
- 50 S. Peng, C. Wang, J. Xie and S. Sun, *J. Am. Chem. Soc.*, 2006, **128**, 10676–10677.
- 51 T.-J. Yoon, H. Lee, H. Shao and R. Weissleder, *Angew. Chem., Int. Ed.*, 2011, **50**, 4663–4666.
- 52 M. N. Nadagouda, A. B. Castle, R. C. Murdock, S. M. Hussain and R. S. Varma, *Green Chem.*, 2010, **12**, 114–122.
- 53 N. Ridley and H. Stuart, *Br. J. Appl. Phys.*, 1968, **2**, 1291–1295.
- 54 S. Gota, E. Guiot, M. Henriot and M. Gautier-Soyer, *Surf. Sci.*, 2000, **454–456**, 796–801.
- 55 A. Cabot, V. F. Puentes, E. Shevchenko, Y. Yin, L. Balcells, M. A. Marcus, S. M. Hughes and A. P. Alivisatos, *J. Am. Chem. Soc.*, 2007, **129**, 10358–10360.
- 56 100% water was not tested due to lack of solubility of the substrates used.
- 57 A. Mori, T. Mizusaki, Y. Miyakawa, E. Ohashi, T. Haga, T. Maegawa, Y. Monguchi and H. Sajiki, *Tetrahedron*, 2006, **62**, 11925–11932.